Cerrahpaşa Med J 2026; 50: 1-7 ORIGINAL ARTICLE

Performance of a Machine Learning Model Based on Routinely Collected Radiological and Clinical Data in Predicting Axillary Metastasis in cN0 Early Stage Breast Cancer

Günay Rona[1], Şermin Kökten[2], Tekin Ahmet Serel[3], Ümitcan Yıldız[1], Tamer Baysal[1]

[1]Department of Radiology, University of Health Sciences, Kartal Doktor Lütfi Kırdar Training and Research Hospital, İstanbul, Türkiye
[2]Department of Pathology, University of Health Sciences, Kartal Doktor Lütfi Kırdar Training and Research Hospital, İstanbul, Türkiye
[3]Department of Urology, Süleyman Demirel University School of Medicine, Isparta, Türkiye

Cite this article as: Rona G, Kökten Ş, Serel TA, Yıldız Ü, Baysal T. Performance of a machine learning model based on routinely collected radiological and clinical data in predicting axillary metastasis in cN0 early stage breast cancer. *Cerrahpaşa Med J.* 2026, 50, 0100, doi: 10.5152/cjm.2026.25100.

What is already known on this topic?

- *Artificial intelligence (AI) achieves successful outcomes in the diagnosis of breast cancer by utilizing multiple imaging modalities.*
- *In breast cancer, the diagnosis of axillary lymph node metastasis (ALNM) is currently established through sentinel lymph node biopsy (SLNB), and less invasive diagnostic techniques are being investigated.*

What does this study add to this topic?

- *In this study, an AI model developed using routinely employed mammography (MG), ultrasonography (US), and tru-cut biopsy results from the primary lesion achieved an AUC of 0.73, an accuracy of 0.68, a recall of 0.60, a precision of 0.67, and an F1 score of 0.62, successfully predicting axillary metastasis.*

Abstract

Objective: Axillary lymph node metastasis (ALNM) is one of the main factors determining treatment and prognosis in breast cancer. This study presents a machine learning (ML) model for the prediction of pretreatment ALNM based on tru-cut biopsy results and the radiological characteristics of the tumor.

Methods: The mammography (MG) and ultrasound (US) findings of patients diagnosed with invasive breast cancer who underwent sentinel lymph node biopsy (SLNB) between 2017 and 2024 were examined, along with the histopathological characteristics of the tumors.

Results: A total of 361 patients were included in the study, with a median age of 52 years (43-64 years) and median lesion size of 24 mm (16-36 mm). While 52.9% of the patients (191) had no ALNM, 47.1% (170) presented with metastasis. Among the evaluated models, LightGBM (AUC: 0.73, accuracy: 0.68) and XGBoost (AUC: 0.734, accuracy: 0.654) successfully predicted axillary metastasis.

Conclusion: The ML model developed using MG, US, and tru-cut biopsy results commonly used in daily practice successfully predicted ALNM.

Keywords: Artificial intelligence, breast cancer, lymphatic metastasis, mammography, machine learning, ultrasound

Introduction

Breast cancer is the most commonly diagnosed form of cancer in women and the most common cause of all cancer-related deaths, accounting for 6.9% of all cases.[1] The 5-year survival rate is reported to be 91.2%.[2] Its morphology, clinical and biological behavior, as well as response to treatment can vary considerably. Age, tumor size, lymph node status, lymphovascular invasion, proliferation markers, and receptor status are considered among the most significant prognostic and predictive markers.[3] Treatment is managed according to the stage, as determined by tumor size, lymph node involvement, receptor status, and the presence of distant metastases.[4] Previous studies have reported young age, larger tumor size, high histological grade, HER2 positivity, central/nipple localization, lymphovascular invasion, and African-American ethnicity to be risk factors for axillary lymph node metastasis (ALNM).[5]

Lymph node involvement is one of the main criteria determining treatment and prognosis, with survival rates decreasing in patients with lymph node involvement.[6] Axillary lymph node dissection (ALND) has been historically performed as a radical procedure but is associated with such significant morbidities as pain, nerve damage, lymphedema, and restricted mobility, making it extremely uncomfortable for the patient. In recent years, sentinel lymph node biopsy (SLNB) has been recognized as a less invasive procedure, offering survival outcomes comparable to ALND and a significant reduction in morbidity rates.[7] The treatment, however, comes with several drawbacks, including

Received: November 25, 2025 **Revision Requested:** December 15, 2025 **Last Revision Received:** January 20, 2026
Accepted: February 3, 2026 **Publication Date:** May 4, 2026
Corresponding author: Günay Rona, Department of Radiology, University of Health Sciences Kartal Doktor Lütfi Kırdar Training and Research Hospital, Kartal, İstanbul, Türkiye **e-mail:** gunayrona@gmail.com
DOI: 10.5152/cjm.2026.25100

Content of this journal is licensed under a Creative Commons Attribution-NonCommercial 4.0 International License.

false-negative rates, the risk of vascular and nerve damage, and reliance on the surgeon's experience. Although less invasive methods have been developed, axillary staging and management remain complex and challenging,[8,9] and so the search for non-invasive and more practical methods is continuing.

Artificial intelligence (AI) has recently shown significant potential in the field of medicine in the analysis of datasets, providing valuable insights into disease diagnosis, treatment, and prognosis prediction. Machine learning (ML) is a branch of AI in which models are being developed that allow the recognition and prediction of patterns in data.[10] Machine learning (ML) methods have yielded successful results in the diagnosis, classification, and treatment monitoring of breast cancer.[11] In addition to the advances in these areas, successful algorithms have been developed for axillary staging that make use of clinical features, radiological images, and histopathological data.[12]

We present here a ML model that predicts axillary metastasis using radiological and pathological features commonly employed in daily practice.

Methods

Data Collection

A total of 650 patients newly diagnosed with invasive breast cancer between 2017 and 2024 were evaluated retrospectively. Ethics committee approval was received from the ethics committee of University of Health Sciences, Kartal Dr. Lütfi Kırdar City Hospital (Approval No.: 202410l0.99/5/16; Date: June 8, 2024). Due to the retropective design of the study and the use of anonymized patient data, the requirement for informed consent was waived by the Instutional Review Board. Excluded from the study were patients who received neoadjuvant chemotherapy, as well as those with bilateral breast cancer, those diagnosed with ductal carcinoma in situ (DCIS), and those with inaccessible pathology results. The mammography (MG), ultrasonography (US), and tru-cut biopsy results of patients meeting the inclusion criteria were evaluated. Mammography examinations were performed in the mediolateral oblique and craniocaudal positions using a Siemens Mammomat Inspiration Prime device. The images were captured by technicians with 1-15 years of experience in mammography. The US images were obtained using a Toshiba Aplio 500 device.

The MG and US examination results were evaluated by a radiologist with 9 years of experience in breast imaging. The patients' age, tumor laterality, histological diagnosis and grade, tumor size, number of lesions, tumor quadrant, distance from the nipple, presence of lymphedema, presence of mass and calcification, the contour characteristics of the lesions on US, the cortex thickness of the most suspicious lymph node in the axilla, receptor status, and molecular subtypes were evaluated.

The lesions' largest diameter, contour characteristics, distance to the nipple, and cortex thickness of the axillary lymph nodes were measured on US. In patients with multiple lesions, the diameter of the largest lesion was recorded. The contour features were divided into 4 groups: well-defined, angular or microlobulated, indistinct, and spiculated. Since a lymph node cortex thickness of ≥ 3 mm increases the likelihood of metastasis, patients were divided into 2 groups: those with a cortex thickness ≥ 3 mm and those with a cortex thickness < 3 mm.[13] The quadrant in which the lesion was located was determined from the US and MG findings, the presence of lymphedema was assessed through mammography, and the presence of diffuse skin thickening and trabecular thickening was considered indicative of lymphedema.

Tru-cut biopsies were performed using a 14G needle under US guidance by a single radiologist, and the specimens were evaluated by a pathologist with 15 years of experience in breast pathology. Histological grade was assessed using the Elston and Ellis method, while receptor status was evaluated through an immunohistochemical analysis. HER-2 scores of 1 were classified as negative, while scores of 3 were classified as positive. For those with a score of 2, the final status was determined using fluorescence in situ hybridization. Estrogen receptors (ER), progesterone receptors (PR), and HER-2 statuses were categorized as positive or negative. Given that a Ki-67 level of ≥ 20% is considered indicative of high proliferative activity and poor prognosis, patients were stratified into 2 groups based on a cutoff value of 20%.[14] Estrogen receptors– and/or PR-positive and HER-2–negative patients were classified as Luminal A; ER- and/or PR-positive and HER-2-positive patients were classified as Luminal B; ER-negative, PR-negative, and HER-2-positive patients were classified as HER-2 enriched; and ER-negative, PR-negative, and HER-2-negative patients were classified as triple negative.

Statistical Analysis

Statistical analyses were conducted using IBM SPSS Statistics version 25.0. (IBM SPSS Corp.; Armonk, NY, USA). A Kolmogorov–Smirnov test was used to assess the fit of quantitative variables to a normal distribution. Descriptive statistics for quantitative variables with a normal distribution were expressed as mean ± standard deviation; descriptive statistics for quantitative variables without a normal distribution were presented as median (25th-75th percentile); descriptive statistics for categorical variables were presented as frequencies (n) and percentages. A *P*-value of less than .05 was considered statistically significant.

Data Preprocessing and Feature Engineering

All data preprocessing, model training, and statistical analyses were performed using Python (version 3.11) with the scikit-learn, pandas, XGBoost, and LightGBM libraries.

Categorical variables of a nominal type were transformed using one-hot encoding to prevent the assumption of an ordinal relationship, expanding the feature space to 35 predictors. Binary features such as tumor side were encoded as 0 and 1. To manage influential observations in the 2 continuous variables,a concise grid-based threshold search and selected the pair that maximized 10-fold cross-validated AUC (with recall/F1 monitored) was performed. The resulting rule excluded records with tumor diameter ≥55 mm or distance from the nipple ≥130 mm. This single rule was applied uniformly before modeling, removing 15 patients (4.0%) and leaving 361 for analysis. All subsequent preprocessing (encoding and scaling) was fitted within each training fold to avoid data leakage.

Model Development and Evaluation Strategy

To assess the model's performance, a 10-fold stratified cross-validation approach was employed. The stratification ensured that the proportion of patients with and without ALNM was preserved in each fold, reducing the risk of sampling bias. To avoid data leakage, preprocessing was incorporated into machine-learning pipelines. Within each fold, continuous variables were standardized to z-scores (mean = 0, standard deviation = 1) using parameters derived exclusively from the training data.

Eight machine-learning algorithms were tested: Logistic Regression, Random Forest, XGBoost, LightGBM, Support Vector Machine (SVM), k-Nearest Neighbors (KNN), Gaussian Naive Bayes, and a Multi-Layer Perceptron (MLP) neural network. These models were selected to represent diverse methodological

paradigms, including linear, ensemble, kernel-based, probabilistic, distance-based, and neural architectures. All models were implemented with their default hyperparameters, except for minor adjustments (e.g., Random Forest with 100 trees, LightGBM with 50 estimators and 20 leaves), to ensure a standardized yet fair comparison.

Performance Metrics and Statistical Analysis

Model performance was assessed using accuracy, precision, recall, F1-score, and the area under the receiver-operating characteristic curve (AUC). All metrics were reported as the mean and standard deviation across the 10 folds of cross-validation. Accuracy was included as a general measure of overall correctness, while Recall and AUC were emphasized as the primary indicators of clinical utility, given the importance of minimizing false negatives in detecting metastatic patients.

Results

Data from a total of 601 patients were analyzed, and 124 patients who received neoadjuvant chemotherapy, 36 with inaccessible SLNB results, 42 with incomplete pathology and clinical results, 18 with recurrence, and 5 with bilateral breast cancer were excluded from the study. In addition, 15 patients were excluded from the study by performing threshold value screening within the scope of data pre-processing because they had extreme values in the ML process. Subsequently, a total of 361 patients with a median age of 54 years (45-66 years) were included in the study. The median lesion size was 20 mm (15-30 mm); the median distance from the nipple was 46 mm (24-70 mm); no ALNM was present in 52.9% of the patients (191) while 47.1% (170) had ALNM. The characteristics of the patients are detailed in Table 1.

Ensemble learners provided the strongest overall discrimination. In Figure 1, the performances of all models are presented. LightGBM achieved a good AUC (0.736 ± 0.085) with a relatively balanced secondary performance profile (accuracy: 0.681 ± 0.091; precision: 0.675; recall: 0.600 ± 0.160; F1-score: 0.626) (Figures 2 and 3). XGBoost showed nearly equivalent discrimination (AUC 0.734 ± 0.085) with slightly lower accuracy (0.654 ± 0.058) and a similar balance of precision (0.626) and recall (0.619 ± 0.110; F1-score 0.617). Random Forest ranked next by AUC (0.707 ± 0.077) yet delivered the highest F1-score overall (0.628), reflecting a solid compromise between precision (0.674) and recall (0.593 ± 0.104); its accuracy (0.681 ± 0.077) was comparable to LightGBM.

The linear baseline, Logistic Regression, performed competitively given its simplicity (AUC 0.701 ± 0.087; accuracy 0.673 ± 0.081; precision 0.668; recall 0.576 ± 0.116; F1-score 0.614). Models differed in clinically relevant error profiles. Gaussian Naive Bayes yielded the highest recall (0.642 ± 0.111) despite a modest AUC (0.684 ± 0.100) and accuracy (0.646 ± 0.076), suggesting potential utility where minimizing false negatives is prioritized. In contrast, the Support Vector Machine attained the highest precision (0.695) with an AUC of 0.693 ± 0.084 and accuracy of 0.670 ± 0.081, but at the expense of markedly lower recall (0.515 ± 0.156), which may limit its suitability when high recall is required.

Neural and distance-based methods were less effective on this dataset. The multi-layer perceptron (AUC 0.643 ± 0.106; accuracy 0.623 ± 0.084; precision 0.611; recall 0.556 ± 0.114) and k-nearest neighbors (AUC 0.563 ± 0.084; accuracy 0.560 ± 0.058; precision 0.531; recall 0.450 ± 0.087) consistently underperformed across metrics, indicating that the pattern structure in these features is better captured by tree-based ensembles than by fully connected or distance-based classifiers.

Because the class distribution was near-balanced (47%/53%), accuracy values were broadly similar among the top models and less discriminative than AUC and recall for clinical interpretation. Taken together, LightGBM—and, secondarily, XGBoost—offer the best overall discrimination with favorable precision–recall tradeoffs. Gaussian Naive Bayes may be preferred in recall-critical settings. The operating point could be further optimized via threshold tuning according to clinical priorities, and future work should include external validation to confirm generalizability.

Discussion

In this study,a successful ML model using tru-cut biopsy results and radiological features of the tumor used in patients with invasive breast cancer was developed. LightGBM and XGBoost successfully predicted axillary metastasis with acceptable AUC and accuracy values. However, the recall values were relatively low, indicating considerable variability across cross-validation folds and reduced model stability. The recall value was relatively low, indicating considerable variability across cross-validation folds and reduced model stability. The relatively large standard deviations observed in the cross-validation results are likely attributable to variations in sample composition across different folds, which is expected in studies with limited sample sizes and heterogeneous patient populations. Despite this variability, the model demonstrated consistent overall performance across cross-validation iterations, supporting its robustness within the current dataset. These results suggest that the model maintains stable predictive capability, while future validation in larger and more diverse cohorts may further strengthen its generalizability.

In previous studies, ML models were created using clinical, radiological, and pathological findings. The model developed by Shahriarirad et al[15] based on variables such as age, family history, pregnancy, and breastfeeding data, number of miscarriages and live births, receptor status, tumor stage, histology, multicentricity, tumor size, lymphovascular invasion, and DCIS percentage predicted ALNM with 75% accuracy, 81% sensitivity, 70% specificity, 87% sensitivity, and 0.74 AUC. The model created by Polat et al[16] with clinicopathological features such as age, race, tumor size, ER, HER-2, Ki-67, and grade achieved an AUC of 0.63, sensitivity of 75%, specificity of 52%, and false-negative rate of 65%. In a study, Chen et al[17] applied a clinical model incorporating age, histological grade, molecular subtype, BI-RADS category, tumor size, and lymph node status on magnetic resonance imaging (MRI) achieved an AUC of 0.669, 55.7% accuracy, 76.4% sensitivity, and 48.0% specificity. In a study by Zhang et al[18], a decision tree model developed using tumor size, subcutaneous adipose tissue infiltration, interstitial adipose tissue infiltration, and tumor quadrant location was able to predict ALN metastasis with an accuracy of 69.52%. In a study by Hassan et al[19], advanced disease stage, age, family history, margin status, and ER/PR positivity were associated with sentinel lymph node metastasis, and the model they developed predicted ALNM with an AUC of 0.70, 84% accuracy, 61% sensitivity, and 62% specificity. In another study, progesterone receptor (PR) negativity, race, age, lobular carcinoma, micropapillary DCIS, axillary tail tumor location, poor differentiation, and larger tumor diameter were found to be associated with ALNM in T1 stage breast cancer cases, and the nomogram created based on these features successfully predicted axillary metastasis with an AUC of 0.739, a sensitivity of 65.78%, and a specificity of 69.99%.[20] A model developed using axillary US findings, maximum tumor diameter, molecular subtypes, and lymphovascular invasion predicted ALNM with an AUC of 0.793.[21] In this study,

Table 1. Characteristics of Patients by Groups

		All Patients	ALNM Negative	ALNM Positive
Age (median, Q1, Q2)		54 (45, 66)	55 (46,66)	52 (40, 65)
Lesion diameter (median, Q1, Q2)		20 (15, 30) mm	20 (11, 28)	23 (15, 35)
Nipple distance (median, Q1, Q2)		41 (18, 65) mm	50 (30, 75)	40 (20, 67)
Tumour side, N (%)	Right	176 (48.8)	101 (51.5)	75 (45.5)
	Left	185 (51.2)	95 (48.5)	90 (54.5)
Quadrant, N (%)	Upper outer	128 (35.5)	65 (33.2)	63 (38.2)
	Upper inner	75 (20.8)	52 (26.5)	23 (13.9)
	Lower outer	39 (10.8)	19 (9.7)	20 (12.1)
	Lower inner	25 (6.9)	13 (6.6)	12 (7.3)
	Central/nipple	10 (2.8)	4 (2.0)	6 (3.6)
	Overlap quadrant	57 (15.8)	30 (15.3)	27 (16.4)
	Axillary tail	8 (2.2)	5 (2.6)	3 (1.8)
	Multiple	19 (5.3)	8 (4.1)	11 (6.7)
Histological type, N (%)	Invasive ductal carcinoma, NST	316 (87.5)	168 (85.7)	148 (89.7)
	Invasive lobulary carcinoma	19 (5.3)	10 (5.1)	9 (5.5)
	Musinous carcinoma	6 (1.7)	3 (1.5)	3 (1.8)
	Other type	20 (5.5)	15 (7.7)	5 (3.0)
Lesion number, N (%)	Single	284 (78.7)	167 (85.2)	117 (70.9)
	Multiple	77 (21.3)	29 (14.8)	48 (29.1)
Lesion type, N (%)	Mass	274 (75.9)	155 (79.1)	119 (72.1)
	Calcification	5 (1.4)	4 (2.0)	1 (0.6)
	Mass and calcification	82 (22.7)	37 (18.9)	45 (27.3)
Lymphedema, N (%)	No	345 (95.6)	193 (98.5)	152 (92.1)
	Yes	16 (4.4)	3 (1.5)	13 (7.9)
Histological grade, N (%)	1	92 (25.5)	55 (28.1)	37 (22.4)
	2	214 (59.3)	112 (57.1)	102 (61.8)
	3	55 (15.2)	29 (14.8)	26 (15.8)
Estrogen receptor, N (%)	Negative	35 (9.7)	19 (9.7)	16 (9.7)
	Positive	326 (90.3)	177 (90.3)	149 (90.3)
Progesterone receptor, N (%)	Negative	82 (22.7)	45 (23.0)	37 (22.4)
	Positive	279 (77.3)	151 (77.0)	128 (77.6)
Her-2 receptor, N (%)	Negative	241 (66.8)	130 (66.3)	111 (67.3)
	Positive	120 (33.2)	66 (33.7)	54 (32.7)
Ki 67 level, N (%)	<20	146 (40.4)	86 (43.9)	60 (36.4)
	>20	215 (59.6)	110 (56.1)	105 (63.6)
Molecular subtype, N (%)	Luminal A	208 (57.6)	112 (57.1)	96 (58.2)
	Luminal B	118 (32.7)	65 (33.2)	53 (32.1)
	Her-2	15 (4.2)	8 (4.1)	7 (4.2)
	Triple negative	20 (5.5)	11 (5.6)	9 (5.5)

ALNM, axillary lymph node metastasis.

10-Fold Cross-Validation Performance of Models (mean ± std. dev.)

Model	AUC	Recall	Precision	F1-score	Accuracy
LightGBM	**0,736 ± 0,085**	0,600 ± 0,160	0,675	0,626	**0,681 ± 0,091**
XGBoost	0,734 ± 0,085	0,619 ± 0,110	0,626	0,617	0,654 ± 0,058
Random_Forest	0,707 ± 0,077	0,593 ± 0,104	0,674	**0,628**	0,681 ± 0,077
Logistic_Regression	0,701 ± 0,087	0,576 ± 0,116	0,668	0,614	0,673 ± 0,081
SVM	0,693 ± 0,084	0,515 ± 0,156	**0,695**	0,578	0,670 ± 0,081
GaussianNB	0,684 ± 0,100	**0,642 ± 0,111**	0,623	0,624	0,646 ± 0,076
MLP	0,643 ± 0,106	0,556 ± 0,114	0,611	0,572	0,623 ± 0,084
KNN	0,563 ± 0,084	0,450 ± 0,087	0,531	0,480	0,560 ± 0,058

Figure 1. 10-Fold cross-validation performance of models

more efficient model relying on routinely employed methods was developed, without incorporating costly and less accessible examinations such as MRI.

In this study, a successful model using age, tumor size, lesion number, distance to the nipple, tumor quadrant, number of lesions, tumor contour features, lymph node cortex thickness, presence of lymphedema, HER-2 status, and Ki-67 levels was obtained. Previous studies have shown that tumor size is associated with ALNM, and that the risk of ALNM increases as tumor size increases.[19] Previous studies have also identified age, HER-2 status, and Ki-67 levels as factors associated with ALN metastasis.[16] Yoshihara et al[22] reported a relationship between ALN metastasis and parameters such as lymphovascular invasion, large tumor diameter, retroareolar and lateral tumor locations, and multiple foci, but no association with age, ER, PR, or HER-2 status. In addition, an association between age and ALN metastasis has been reported in numerous earlier studies.[15-18] Although controversial in the literature, the relationship between HER-2 status,[15,16,18,19,21] Ki-67 levels[16,23] and ALN metastasis has been demonstrated in other studies. In a study by Yang et al[24], the quadrant of the tumor and its distance from the nipple were associated with ALNM. In the study by Zhang et al[18], tumor quadrant was identified as an independent risk factor for ALNM.

The limitations of this study include its retrospective nature and small sample size, the evaluation of imaging findings by a single radiologist, the single-center design, and the absence of external and temporal validation cohorts. In this study, no extensive hyperparameter optimization was performed; models were primarily implemented using default settings with minor, predefined adjustments to ensure a fair and standardized comparison. Although excluding outliers improved internal performance in this study, it may limit prospective applicability. In the analysis, both receptor

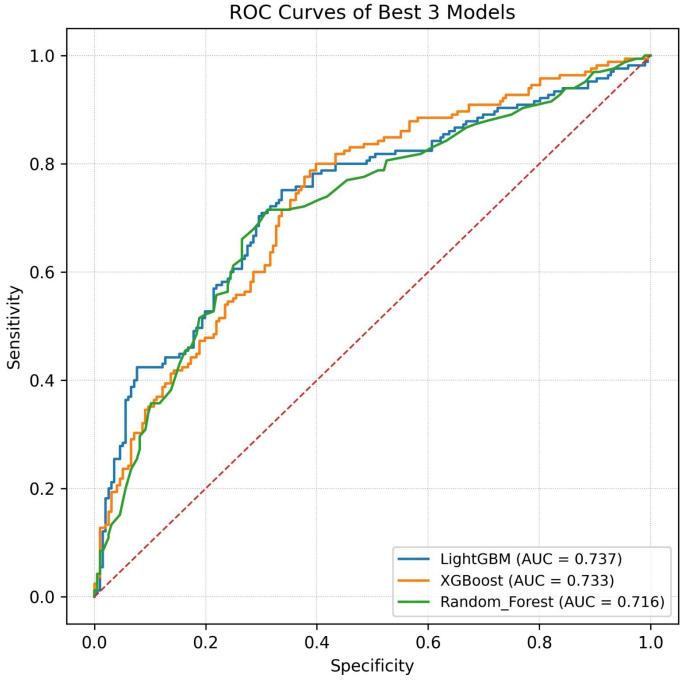


Figure 2. Receiver operating characteristic analysis of LightGBM model in predicting axillary metastasis.

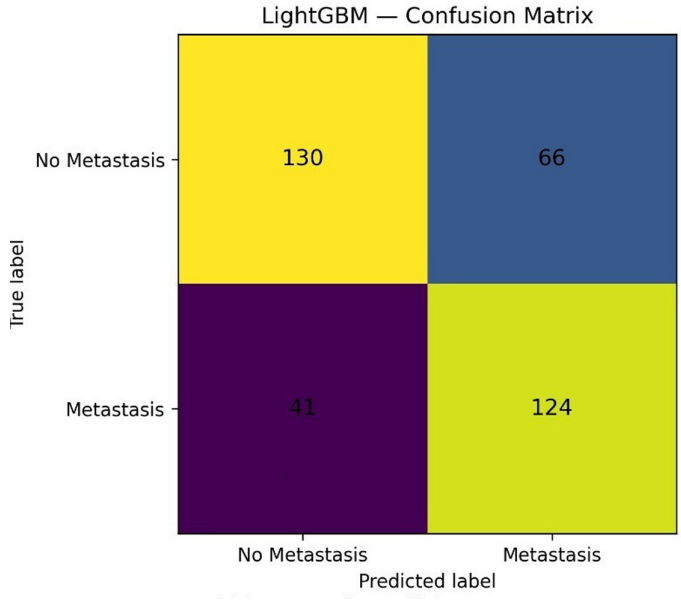


Figure 3. Classification report of the LightGBM model for predicting axillary metastasis.

status and molecular subtypes were included. However, since molecular subtypes are derived from receptor status, their concurrent use may lead to redundancy. Additionally, lymphovascular invasion could not be assessed because the pathological data were derived from tru-cut biopsy specimens.

In conclusion, the model, developed using radiological and pathological characteristics commonly used in daily practice, is shown to be successful in predicting ALNM, and the radiological parameters employed are easily accessible through MG and US, which require no contrast agents and can be readily evaluated by radiologists with limited experience. The model created in the present study can thus provide valuable insights into the prediction of ALNM in daily practice. The model may enable the non-invasive prediction of ALNM and could potentially help identify low-risk patients in whom SLNB might be avoided.

Data Availability Statement: The data that support the findings of this study are available on request from the corresponding author.

Ethics Committee Approval: Ethics committee approval was received for this study from the ethics committee of University of Health Sciences, Kartal Dr. Lütfi Kırdar City Hospital (Approval No.: 202410l0.99/5/16; Date: June 8, 2024).

Informed Consent: Due to the retropective design of the study and the use of anonymized patient data, the requirement for informed consent was waived by the Instutional Review Board.

Peer-review: Externally peer-reviewed.

Author Contributions: Concept – G.R., Ş.K.; Design – G.R., Ş.K.; Supervision – G.R., Ş.K.; Resources – G.R., Ş.K.; Materials – G.R., Ş.K.; Data Collection and/or Processing – G.R., Ş.K.; Analysis and/or Interpretation – G.R., T.A.S., Ü.Y.; Literature Search – G.R., T.A.S., Ü.Y.; Writing Manuscript – G.R., Ü.Y.; Critical Review – G.R., T.B.

Declaration of Generative AI: The authors declared that they did not use generative AI or AI-assisted technologies in the preparation of this manuscript.

Declaration of Interests: The authors have no conflict of interest to declare.

Funding: The authors declared that this study has received no financial support.

References

1. Sung H, Ferlay J, Siegel RL, et al. Global cancer statistics 2020: GLOBOCAN estimates of incidence and mortality worldwide for 36 cancers in 185 countries. *CA Cancer J Clin*. 2021;71(3):209-249. [CrossRef]
2. Tan KF, Adam F, Hussin H, et al.. A comparison of breast cancer survival across different age groups: a multicentric database study in Penang, Malaysia. *Epidemiol Health*. 2021;43:e2021038. [CrossRef]
3. Tarighati E, Keivan H, Mahani H. A review of prognostic and predictive biomarkers in breast cancer. *Clin Exp Med*. 2023;23(1):1-16. [CrossRef]
4. Rosen RD, Sapra A. TNM classification. *StatPearls* [Internet]; Updated 2023. In: Treasure Island (FL): StatPearls Publishing:2024. https://www.ncbi.nlm.nih.gov/books/NBK553187/.
5. Luo M, Lin X, Hao D, et al. Incidence and risk factors of lymph node metastasis in breast cancer patients without preoperative chemoradiotherapy and neoadjuvant therapy: analysis of SEER data. *Gland Surg*. 2023;12(11):1508-1524. [CrossRef]
6. Fernandes JO, Cardoso-Filho C, Kraft MB, et al. Differences in breast cancer survival and stage by age in off-target screening groups: a population-based retrospective study. *AJOG Glob Rep*. 2023;3(2):100208. [CrossRef]
7. Gradishar WJ, Moran MS, Abraham J, et al. Breast cancer, version 3.2022, NCCN clinical practice guidelines in oncology. *J Natl Compr Canc Netw*. 2022;20(6):691-722. [CrossRef]
8. Cortina CS, Yen TWF, Bergom C, et al. Breast cancer-related lymphedema rates after modern axillary treatments: how accurate are our estimates? *Surgery*. 2022;171(3):682-686. [CrossRef]
9. Kataria K, Srivastava A, Qaiser D. What is a false negative sentinel node biopsy: definition, reasons and ways to minimize it? *Indian J Surg*. 2016;78(5):396-401. [CrossRef]
10. Alowais SA, Alghamdi SS, Alsuhebany N, et al. Revolutionizing healthcare: the role of artificial intelligence in clinical practice. *BMC Med Educ*. 2023;23(1):689. [CrossRef]
11. Yan S, Li J, Wu W. Artificial intelligence in breast cancer: application and future perspectives. *J Cancer Res Clin Oncol*. 2023;149(17):16179-16190. [CrossRef]
12. Vrdoljak J, Krešo A, Kumrić M, et al. The role of AI in breast cancer lymph node classification: A comprehensive review. *Cancers (Basel)*. 2023;15(8):2400. [CrossRef]
13. Loonis AT, Chesebro AL, Bay CP, et al. Positive predictive value of axillary lymph node cortical thickness and nodal, clinical, and tumor characteristics in newly diagnosed breast cancer patients. *Breast Cancer Res Treat*. 2024;203(3):511-521. [CrossRef]
14. Davey MG, Hynes SO, Kerin MJ, et al. Ki-67 as a prognostic biomarker in invasive breast cancer. *Cancers*. 2021;13(17):4455. [CrossRef]
15. Shahriarirad R, Meshkati Yazd SM, Fathian R, et al. Prediction of sentinel lymph node metastasis in breast cancer patients based on preoperative features: a deep machine learning approach. *Sci Rep*. 2024;14(1):1351. [CrossRef]
16. Polat DS, Nguyen S, Karbasi P, et al. Machine learning prediction of lymph node metastasis in breast cancer: performance of a multi-institutional MRI-based 4D convolutional neural network. *Radiol Imaging Cancer*. 2024;6(3):e230107. [CrossRef]
17. Chen M, Kong C, Lin G, et al. Development and validation of convolutional neural network-based model to predict the risk of sentinel or non-sentinel lymph node metastasis in patients with breast cancer: a machine learning study. *EClinicalmedicine*. 2023;63:102176. [CrossRef]
18. Zhang Y, Li J, Fan Y, et al. Risk factors for axillary lymph node metastases in clinical stage T1-2N0M0 breast cancer patients. *Med (Baltim)*. 2019;98(40):e17481. [CrossRef]
19. Hassan A, Tamirisa N, Singh P, et al. . A novel support vector machine to predict sentinel lymph node status in elderly patients with breast cancer. *JCO*. 2022;40(16_suppl):1560-1560.[CrossRef]
20. Qian F, Shen H, Deng C, et al. Establishment of a logistic regression model nomogram for clinicopathological characteristics and risk factors with axillary lymph node metastasis in T1 locally advanced breast cancer: a retrospective study. *Gland Surg*. 2024;13(6):871-884. [CrossRef]
21. Zhang Z, Jiang Q, Wang J, et al. A nomogram model for predicting the risk of axillary lymph node metastasis in patients with early breast cancer and cN0 status. *Oncol Lett*. 2024;28(2):345. [CrossRef]
22. Yoshihara E, Smeets A, Laenen A, et al. Predictors of axillary lymph node metastases in early breast cancer and their applicability in clinical practice. *Breast*. 2013;22(3):357-361. [CrossRef]
23. Sun P, Han J, Li M, et al. Spectral ultrasound combined with clinical pathological parameters in prediction of axillary lymph node metastasis in breast cancer. *J Ultrasound Med*. 2024;43(12):2311-2324. [CrossRef]
24. Yang J, Yang Q, Mukherjee A, et al. Distance between the tumour and nipple as a predictor of axillary lymph node involvement in breast cancer. *Cancer Manag Res*. 2021;13:193-199. [CrossRef]